Polyhedron 29 (2010) 1387–1392

Contents lists available at ScienceDirect

Polyhedron

journal homepage: www.elsevier.com/locate/poly

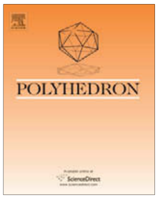

Synthesis, structures and magnetic properties of copper (II) and cobalt (II) complexes containing pyridyl-substituted nitronyl nitroxide and 3,5-dinitrobenzoate

Chen-Xi Zhang [a,*], Yu-Ying Zhang [b], Ya-Qiu Sun [c]

[a] College of Science, Tianjin University of Science and Technology, Tianjin 300457, People's Republic of China
[b] Department of Chemistry, NanKai University, Tianjin 300071, People's Republic of China
[c] Department of Chemistry, Tianjin Normal University, Tianjin 300387, People's Republic of China

ARTICLE INFO

Article history:
Received 12 October 2009
Accepted 30 December 2009
Available online 28 January 2010

Keywords:
Crystal structure
Nitronyl nitroxide metal complexes
Copper(II)/3,5-dinitrobenzoate complexes
Cobalt(II)/3,5-dinitrobenzoate complexes
Magnetism

ABSTRACT

Four new metal-radical complexes - [Cu(NIT3Py)$_2$(DTB)$_2$] **1**, [Co(NIT3Py)$_2$(DTB)$_2$(CH$_3$OH)$_2$] **2**, [Cu(NIT4-Py)$_2$(DTB)$_2$(H$_2$O)$_2$] **3**, [Co(NIT4Py)$_2$(DTB)$_2$(H$_2$O)$_2$] **4**, (NIT3Py = 2-(3$'$-pyridyl)-4,4,5,5-tetramethylimidazoline-1-oxyl-3-oxide], NIT4Py = 2-(4$'$-pyridyl)-4,4,5,5-tetramethylimidazoline-1-oxyl-3-oxide], DTB = 3, 5-dinitrobenzoic anion) have been synthesized by using transition metal ions, nitronyl nitroxide radicals as spin carriers, and incorporating 3,5-dinitrobenzoic acid (DTB) as a coligand.

The structures of **1**–**4** were determined by X-ray single-crystal analyses. Complex **1** has a square planar geometry, where the Cu(II) ion is located in the central site of the rectangle and two radicals and two DTBA ligands are *trans*-coordinated to the Cu(II) ion. The other three complexes (**2-4**) have similar structures, in which two radicals, two DTBA ligands and two solvent molecules act as terminal ligands to form six coordinate distorted octahedrons. The magnetic behaviors of these compounds indicate that antiferromagnetic exchanges exist between the radical ligands and the metal ions, and their magnetic properties are explained by their structures and a magnetic exchange mechanism.

1. Introduction

In the field of molecular-based magnetic materials, much attention has been paid to the coordination of paramagnetic metal ions with nitronyl nitroxide radicals in terms of the "metal-organic" strategy [1,2]. By employment of this strategy, a large number of metal-radical complexes with various structures have been synthesized and magnetically characterized. Some of these complexes exhibit single molecule magnet (SMM) behavior [3] or single chain magnet (SCM) behavior [4].

However, the disadvantage of nitronyl nitroxides is that they are weak Lewis bases; they prefer to coordinate to acidic metal centers, such as hexafluoroacetylacetonato- or trifluoroacetato-metal complexes as starting materials. This has led to the development of functionalized nitronyl nitroxide radicals in which a strong coligand is incorporated. This way has proved to be particularly productive, allowing the coordination of most metal ions without the requirement of electron-withdrawing ancillary ligands. Among them, nitroxides substituted with pyridine groups have the advantage of forming stable chelate complexes with the support of the auxiliary substitute groups [5–8].

In the different geometric structures of Cu(II)-nitronyl nitroxide heterospin systems, the overlap between the Cu(II) magnetic orbital and the π^* magnetic orbital of the radical is favored or forbidden, thus quite different magnetic behaviors (ferromagnetic and antiferromagnetic interactions) are expected [7,9]. Co(II)-nitronyl nitroxide compounds have been investigated rarely due to a large spin-orbital coupling, although the Co(II) ion is a very effective spin carrier [4,12]. Fundamental magneto-structural correlation studies of Cu(II) and Co(II) nitronyl nitroxides are necessary [9–14], especially for investigating how the structural factors affect the metal-radical interactions. Such investigations are necessary not only for understanding the magnetic exchange mechanism between the metal and organic radical but also for guiding the design of new organic radical ligands for the development of novel molecular magnetic materials. On the other hand, 3,5-dinitrobenzoic acid (DTB), containing a carboxylic group, can coordinate to metal ions with a great flexibility in the chemical design of molecular assemblies [15–18].

Along this line, taking advantage of the abilities of both nitroxide radicals and DTB (the 3,5-dinitrobenzoic anion) to coordinate to transition metals, we have synthesized four metal-radical complexes: [Cu(NIT3Py)$_2$(DTB)$_2$] **1**, [Co(NIT3Py)$_2$(DTB)$_2$(CH$_3$OH)$_2$] **2**, [Cu(NIT4Py)$_2$(DTB)$_2$(H$_2$O)$_2$] **3** and [Co(NIT4Py)$_2$(DTB)$_2$(H$_2$O)$_2$] **4**.

---

* Corresponding author. Tel.: +86 22 23500383; fax: +86 22 23502082.
E-mail addresses: zcx@tust.edu.cn, zcx@mail.nankai.edu.cn (C.-X. Zhang).

0277-5387/$ - see front matter © 2010 Elsevier Ltd. All rights reserved.
doi:10.1016/j.poly.2009.12.039

Table 1
Crystallographic and refinement data for complexes **1**, **2**, **3** and **4**.

	1	**2**	**3**	**4**
Empirical formula	$C_{38}H_{38}CuN_{10}O_{16}$	$C_{40}H_{46}CoN_{10}O_{18}$	$C_{38}H_{42}CuN_{10}O_{18}$	$C_{38}H_{42}CoN_{10}O_{18}$
Formula weight	954.32	1013.80	990.36	985.75
Crystal system	triclinic	triclinic	triclinic	triclinic
Space group	$P\bar{1}$	$P\bar{1}$	$P\bar{1}$	$P\bar{1}$
a (Å)	7.129(11)	8.7646(16)	10.123(3)	10.110(4)
b (Å)	11.892(19)	10.962(2)	10.198(3)	10.290(3)
c (Å)	12.567(16)	12.626(2)	10.810(3)	10.656(4)
α (°)	87.85(3)	75.387(4)	78.517(4)	79.004(5)
β (°)	75.644(15)	75.736(4)	85.848(5)	87.806(5)
γ (°)	88.98(4)	75.486(4)	85.374(4)	85.999(6)
V (Å$^{3)}$	1031(3)	1114.4(4)	1088.2(5)	1085.1(6)
Z	1	1	1	1
Calculated density (g cm$^{3)}$	1.536	1.511	1.511	1.508
Absorption coefficient (mm$^{-1)}$	0.616	0.474	0.590	0.484
Crystal size (mm)	0.32 × 0.26 × 0.22	0.20 × 0.16 × 0.14	0.18 × 0.14 × 0.12	0.35 × 0.25 × 0.20
θ Range for data collection (°)	1.77–25.00	1.96–26.41	2.02–26.45	2.02–26.42
Reflections collected	2441	6445	6388	6324
Independent reflection	2433 [R(int) = 0.1088]	4502 [R(int) = 0.0147]	4436 [R(int) = 0.0325]	4406 [R(int) = 0.0166]
Final *R* indices [$I > 2\sigma(I)$]	R_1[a] = 0.0803, wR_2[b] = 0.1831	R_1 = 0.0514, wR_2 = 0.1449	R_1 = 0.0517, wR_2 = 0.0921	R_1 = 0.0360, wR_2 = 0.0819

[a] $R_1 = \Sigma||F_o|-|F_c||/\Sigma|F_o|$.
[b] $wR_2 = \Sigma\{[w(F_o^2-F_c^2)^2]/\Sigma[wF_o^2]^2\}^{1/2}$.

Herein the synthesis, X-ray structures and magnetic properties of these complexes are reported.

Table 2
Selected bond lengths (Å) and angles (°) for complexes **1–4**.

Complex **1**		*Complex* **2**	
Cu(1)–O(3)	1.974(6)	Co(1)–O(3)	1.963(2)
Cu(1)–N(1)	2.001(7)	Co(1)–N(1)	2.024(2)
N(2)–O(1)	1.265(9)	Co(1)–O(9)	2.404(4)
O(2)–N(3)	1.31(1)	N(2)–O(1)	1.268(3)
O(3)–Cu(1)–N(1)	90.5(2)	O(3)–Co(1)–N(1)	91.14(9)
C(13)–O(3)–Cu(1)	105.2(5)	O(3)–Co(1)–O(9)	83.4(1)
C(1)–N(1)–Cu(1)	123.7(6)	N(1)–Co(1)–O(9)	91.9(1)
Complex **3**		*Complex* **4**	
Cu(1)–O(3)	1.995 (2)	Co(1)–O(3)	2.079(1)
Cu(1)–N(1)	2.020(2)	Co(1)–N(1)	2.146(2)
Cu(1)–O(9)	2.317(2)	Co(1)–O(9)	2.095(2)
N(2)–O(1)	1.277(3)	N(2)–O(1)	1.285(2)
O(3)–Cu(1)–N(1)	92.53(8)	O(3)–Co(1)–N(1)	92.27(6)
O(3)–Cu(1)–O(9)	89.46(8)	O(3)–Co(1)–O(9)	89.69(5)
N(1)–Cu(1)–O(9)	92.59(9)	N(1)–Co(1)–O(9)	85.90(6)

2. Experimental

2.1. General

All reagents were purchased from commercial sources and were used as received. Elemental analyses for carbon, hydrogen and nitrogen were carried out on a Model 240 Perkin-Elmer elemental analyzer. The infrared spectra were recorded on a Shimadzu IR spectrophotometer model 408 in the 4000–600 cm^{-1} region, using KBr pellets. The UV–Vis spectra were recorded on a UV-2101 PC spectrophotometer in the 190–800 nm regions. Temperature dependent magnetic susceptibilities were measured on a MPMS-7 SQUID magnetometer. Diamagnetic corrections were made with Pascal's constants for all constituent atoms.

2.2. Synthesis

2-(3′-Pyridyl)-4,4,5,5-tetramethylimidazoline-1-oxyl-3-oxide and 2-(4′-pyridyl)-4,4,5,5-tetramethylimidazoline-1-oxyl-3-oxide were prepared according to the literature method [19,20].

[Cu(NIT3Py)$_2$(DTB)$_2$] **1** was synthesized by adding 5 mL aqueous solution of potassium 3,5-dinitrobenzoate (0.101 g, 0.4 mmol) into a mixed solution of Cu(OAc)$_2$·H$_2$O (0.040 g, 0.2 mmol) and NIT3Py (0.094 g, 0.4 mmol) in 15 mL methanol. The mixture was stirred for 1 h and then filtered, and the clear blue filtrate was kept at room temperature for three days. Green crystals were obtained. *Anal.* Calc. for $C_{38}H_{38}CuN_{10}O_{16}$: C, 47.80; H, 3.98; N, 14.68. Found: C, 47.26; H, 4.16; N, 14.72%. IR (KBr, cm^{-1}): 3096, 1621, 1541, 1454, 1423, 1387, 1343, 1169, 1070, 868, 725, 543.

Blue crystals of [Co(NIT3Py)$_2$(DTB)$_2$(CH$_3$OH)$_2$] **2** were prepared in a manner similar to that of **1** only by replacing Cu(OAc)$_2$·H$_2$O with Co(OAc)$_2$·H$_2$O. *Anal* Calc. for $C_{40}H_{46}CoN_{10}O_{18}$: C, 47.38; H, 4.54; N, 13.82. Found: C, 47.21; H, 4.58; N, 13.90%. IR (KBr, cm^{-1}): 3096, 1652, 1541, 1454, 1423, 1371, 1343, 1169, 1082, 915, 868, 725, 543.

Blue crystals of [Cu(NIT4Py)$_2$(DTB)$_2$(H$_2$O)$_2$] **3** were prepared in a manner similar to that of **1** only by replacing NIT3Py with NIT4Py. *Anal* Calc. for $C_{38}H_{42}CuN_{10}O_{18}$: C, 46.06; H, 4.24; N, 14.14. Found: C, 45.90; H, 4.16; N, 14.32%. IR (KBr, cm^{-1}): 3104, 1625, 1538, 1454, 1383, 1343, 1312, 1161, 1066, 868, 820, 729, 543.

Blue crystals of [Co(NIT4Py)$_2$(DTB)$_2$(H$_2$O)$_2$] **4** were prepared in a manner similar to that of **2** only by replacing NIT3Py with NIT4Py. *Anal*Calc. for $C_{38}H_{42}CoN_{10}O_{18}$: C, 46.29; H, 4.26; N, 14.21. Found: C, 46.42; H, 4.37; N, 14.23%. IR (KBr, cm^{-1}): 3014, 2906, 1609, 1538, 1454, 1379, 1347, 1169, 1066, 911, 864, 725, 547.

2.3. X-ray crystallographic study

Single crystal X-ray diffraction measurements were carried out on a Bruker Smart 1000 diffractometer equipped with graphite-monochromated Mo Kα radiation (λ = 0.71073 Å). Data were collected at room temperature by the φ–ω scan technique in the range 2.27° ≤ θ ≤ 25.02°. The collected data were reduced by using the program SAINT [21] and empirical absorption correction was done by using the SADABS program [22]. The structures were solved with direct methods of SHELXS-97 [23]. The H atoms were assigned with common isotropic displacement factors and included in the final refinement by using geometrical restraints. A full-matrix

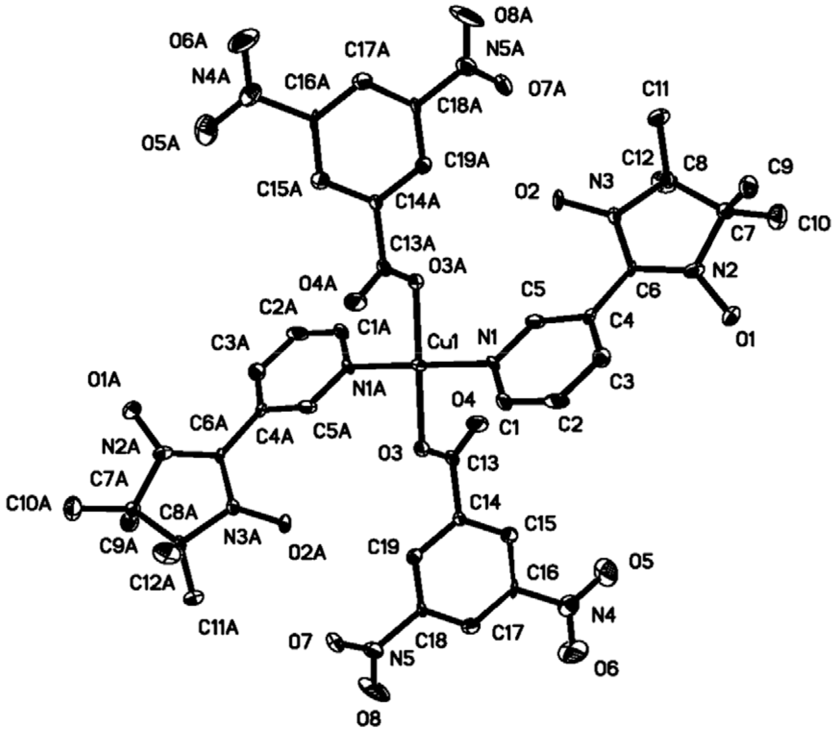

Fig. 1. The molecular structure of the complex [Cu(NIT3Py)$_2$(DNB)$_2$], **1** (hydrogen atoms have been omitted for clarity).

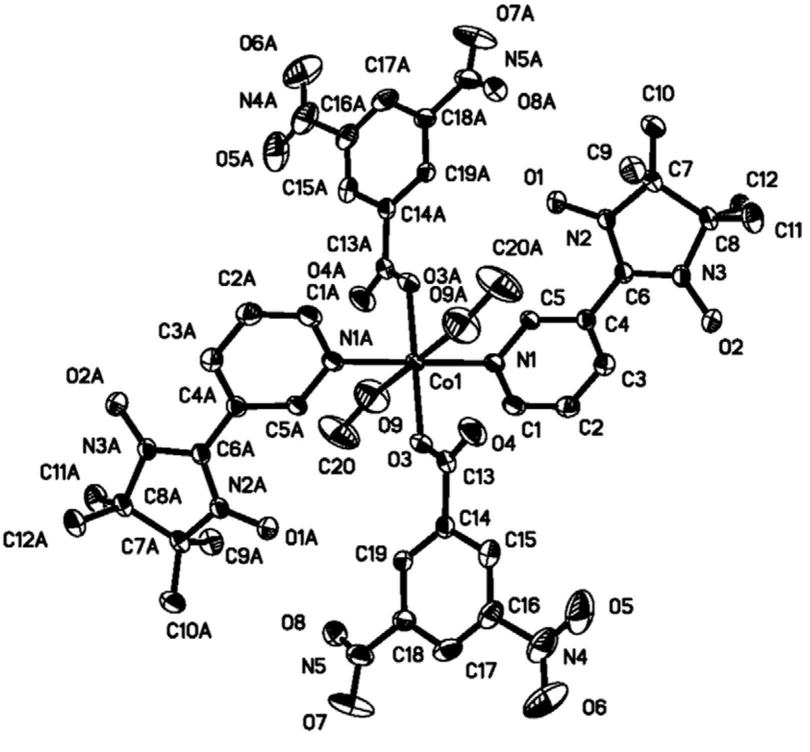

Fig. 2. The molecular structure of the complex [Co(NIT3Py)$_2$(DTB)$_2$(CH$_3$OH)$_2$], **2** (hydrogen atoms have been omitted for clarity).

least-squares refinement on F^2 was carried out using SHELXL-97 [24]. All non-hydrogen atoms were readily located and refined with anisotropic thermal parameters; $R_1 = \Sigma(||F_0|-|Fc||)/\Sigma|F_0|$ and $wR_2 = (\Sigma(|F_0|^2-|F_c|^2)^2/(\Sigma w|F_0|^2)^2$, respectively. Crystal data and selected structural parameters were summarized in Tables 1 and 2, respectively.

3. Results and discussion

3.1. Description of the crystal structures

For complexes **1**, **2**, **3** and **4**, the metal atoms are located on inversion centers. All compounds are in the triclinic space group

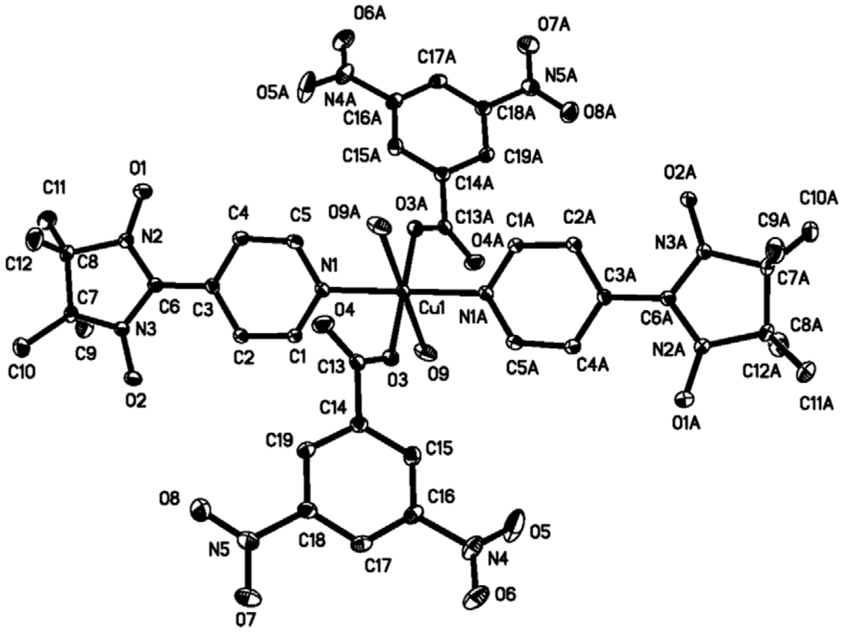

Fig. 3. The molecular structure of the complex $[Cu(NIT4Py)_2(DTB)_2(H_2O)_2]$, **3** (hydrogen atoms have been omitted for clarity).

$P\bar{1}$. For all compounds, either square planar or octahedral coordination geometries are adopted.

An ORTEP drawing of complex **1** is shown in Fig. 1. The Cu(II) ion is four-coordinated in a square planar CuN_2O_2 coordination environment, in which the coordination sites are occupied by two nitrogen atoms (N1, N1A) from NIT3Py anions and two oxygen atoms (O3,O3A) from NTB anions. The Cu–N and Cu–O bond lengths (2.001(7) and 1.974(6) Å) are comparable with those observed in other Cu- NIT3Py complexes [7,28]. The N2–O1 distance (1.265(9) Å) is intermediate among those observed in copper complexes with coordinated NIT3Py radicals [7,9]. The fragment O1–N2–C6–N3–O2 is nearly planar, and forms a dihedral angle of 35.8° with the plane of the pyridine ring.

The crystal structure of complex **2** is illustrated in Fig. 2. The Co(II) ion adopts an octahedral coordination arrangement. Two nitrogen atoms (N1, N1A) from the pyridine rings of the NIT3Py ligands, with a Co–N bond length of 2.024(2) Å, and two oxygen atoms (O3, O3A) from two DTB anions, with a Co–O bond length of 1.963(2) Å, form the equatorial plane of the octahedral geometry. The axial positions of the octahedron are occupied by two oxygen atoms (O9, O9A) from two methanol molecules, with a Co–O bond distance of 2.404(4) Å, which is significantly longer than the basal distances. The fragment O1–N2–C6–N3–O2 is nearly planar too, but forms a dihedral angle of 40.4° with the plane of the pyridine ring. The N2–O1 distance (1.268(3) Å) is similar to N–O distances already reported in

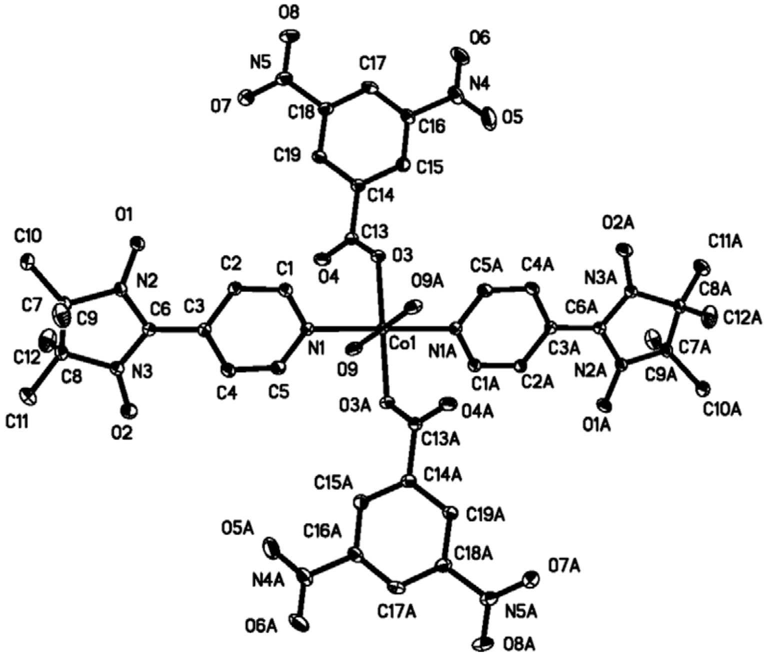

Fig. 4. The molecular structure of the complex $[Co(NIT4Py)_2(DTB)_2(H_2O)_2]$, **4** (hydrogen atoms have been omitted for clarity).

analogous cobalt complexes with coordinated NIT3Py radicals [28,30].

Complex **3** and **4** are isostructural and an ORTEP drawings of complexes **3** and **4** are shown in Figs. 3 and 4. The metal ion is located at an inversion center and adopts a distorted octahedral geometry.

The equatorial plane is formed by two nitrogen atoms from the pyridine rings of NIT4Py ligands and two oxygen atoms from two DTB anions. Two water molecules occupy the apical positions for **3**. However, two oxygen atoms from two DTB anions and two oxygen atoms from two water molecules form the base plane, with two nitrogen atoms from the pyridine rings of NIT4Py ligands occupy the apical positions for **4**. The axial distortion in complex **3** involves the Co–O9 axis whereas that in complex **4** involves the Co–N1 axis. The metal-N (pyridine) bond distances are 2.020(2) and 2.146(2) Å for **3** and **4**, respectively. The metal-O(DTB) bond distances are 1.995(2) for **3** and 2.079(1) Å for **4**, whereas the metal-O(water) bond distances are 2.317(2) and 2.095(2) Å for **3** and **4**, respectively. Thus, similarly to complex **2**, complexes **3** and **4** have an axially distorted octahedral geometry. The axial distortion in complexes **2** and **4** are significantly different in magnitude, with **2** (2.404(4) Å) being more distorted than **4** (2.095(2) Å). The axial distortion in complex **2** involves the Co–O9 axis whereas that in complex **4** involves the Co–N1 axis. These differences maybe are caused by the different kinds of coordinated solvent molecules (methanol and water molecules) and radicals (NIT3Py and NIT4Py). Both the fragments O1–N2–C6–N3–O2 for complex **3** and O1–N2–C6–N3–O2 for complex **4** are nearly planar, but dihedral angles of 12.5° and 7.1° are observed for complexes **3** and **4** with the plane of the pyridine ring, respectively. In the radical ligand, the oxyl bond lengths, the N2–O1 distances 1.277(3) and 1.285(2) Å, are similar to N–O distances already reported in analogous complexes with coordinated NIT4Py radicals [7,31].

3.2. Magnetic properties and discussion

The magnetic susceptibilities, χ_M, for complexes **1**, **2**, **3** and **4** were measured in the 2–300 K region at 10000 G. A typical plot of $\chi_M T$ and χ_M versus T is shown in Fig. 5. The other plots are shown in the Supplementary material.

The $\chi_M T$ value at room temperature is 1.09 $cm^3\,mol^{-1}$ K for complex **1** and 1.07 $cm^3\,mol^{-1}$ K for complex **3**, which are lower than the spin-only value expected for two $S = 1/2$ and one $S = 1/2$ uncoupled spin systems (1.12 $cm^3\,mol^{-1}$ K). When the systems are cooled down, the $\chi_M T$ value decreases, which implies the existence of weak antiferromagnetic spin exchange interactions both in complex **1** and complex **3**.

The magnetic data were fitted into the isotropic model $\hat{H} = -2J(\hat{S}_{Cu}\hat{S}_R + \hat{S}_{Cu}\hat{S}_R)$, where J is the interaction parameter between two paramagnetic centers. For radical–Cu(II)–radical complexes, the theoretical expression of the magnetic susceptibility is

$$\chi_M = \frac{N\beta^2 g^2}{4kT}\left[\frac{1+\exp(-2J/kT)+10exp(J/kT)}{1+\exp(-2J/kT)+2\exp(J/kT)}\right]$$

The best-fitted parameters were $J = -3.18$ cm^{-1}, $g = 1.99$, $R = 1.52 \times 10^{-3}$ for **1** and $J = -8.89$ cm^{-1}, $g = 1.98$, $R = 1.71 \times 10^{-4}$ for **3**, where R is defined as $R = \Sigma[(\chi_M)_{obs} - (\chi_M)_{calc}]^2/\Sigma(\chi_M)^2_{obs}$.

Those above results indicate that an antiferromagnetic exchange exists between the radical and metal ion.

We found the intramolecular metal-radical magnetic couplings varied over a considerably wide range with relatively small structural modifications. This leads to an insight of the magneto-structure relationship.

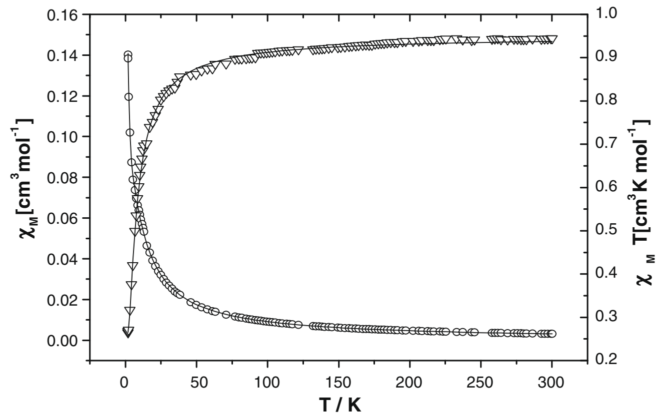

Fig. 5. Experimental and calculated variations of χM (○) and χMT (∇) versus T for [Cu(NIT3Py)2(DTB)2], 1.

In the compound **1**, the O(1)–N(2)–C(6)–N(3)–O(2) mean plane containing the unpaired electron of the radical makes an angle of 32° with the N(1)–Cu(1)–N(1A) plane, and the angle between the N(1)–Cu(1)–N(1A) plane and the plane of the pyridine ring is 39°. These geometrical parameters favor a weak overlap of the π^* magnetic orbital of the radical with the $d_{x^2-y^2}$ magnetic orbital of the Cu(II) ion. This is the origin of the weak antiferromagnetic Cu(II)-nitroxide interaction.

The weak antiferromagnetic interaction between Cu(II) and NIT4Py in compound **3** can be explained by McConnell's mechanism [25], which is shown in Scheme 1. According to this model, a spin distribution would induce a contrary spin on the adjacent atom due to the spin polarization. In the radical ligand, the spin distribution arising from intramolecule spin polarization of the adjacent atoms leads to alternating positive and negative spin density on the carbon backbone of the radical ligand. A large positive spin density is located on the NO groups, while a large negative spin density is located on the sp^2 carbon atom bridging two NO groups, and the alternative delocalization takes place over the pyridine ring due to the spin polarization. This in turn induces a negative spin density on the nitrogen atom of NIT4Py [26,27]. The O(7)–N(2)–C(6)–N(3)–O(8) mean plane containing the unpaired electron of the radical makes an angle of 44.8° with the N(1)–Cu(1)–N(1A) plane. Compared with complex **1**, the large overlap of the π^* magnetic orbital of the radical with the $d_{x^2-y^2}$ magnetic orbital of the planar Cu(II) ion leads to a stronger antiferromagnetic Cu(II)-nitroxide interaction ($J = -8.89$ cm^{-1}). The relevant structural and magnetic data of some Cu(II)-nitroxide complexes are listed in Table 3. It can be seen that when the angle between the O(1)–N(2)–C(6)–N(3)–O(2) plane of the radical and the plane of the pyridine ring is large, an antiferromagnetic exchange interaction is expected, as for the copper complexes with coordinated NIT3Py radicals, however, when the angle between the O(1)–N(2)–C(6)–N(3)–O(2) plane of the radical and the plane of the pyridine ring is small, a weak antiferromagnetic exchange interaction is obtained, as for the copper complexes with coordinated NIT4Py.

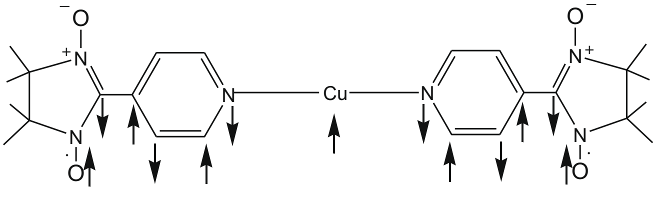

Scheme 1. The spin polarization mechanism for intramolecular magnetic coupling in the compound **3**.

Table 3
Selected structural and magnetic parameters for Cu-NIT3Py and Cu-NIT4Py compounds.

Compound	δ^a (°)	J (cm^{-1})	Reference
$Cu(NITm\text{-}Py)_2(N_3)_2(DMSO)_2$	28.6	3.61	[28]
$Cu(NITmPy)_2(tp)$	6.4	17.0	[32]
$[Cu(Cl_2CHCO_2)_2(NITmPy)_2(H_2O)_2]$	24.91	12.0	[7]
$Cu(NIT3Py)_2(DTB)_2]$	35.8	−3.18	this work
$Cu(NITpPy)_2(NO_3)_2$	30.9	−14.1 ± 0.1	[29]
$Cu(NITpPy)_2(CH_3COO)_2$	29.96	−16.7 ± 0.6	[29]
$Cu(NITpPy)_2[N(CN)_2]_2{\cdot}(H_2O)_2$	29.61	−17.0 ± 0.2	[29]
$[Cu(Cl_3CCO_2)_2(NITpPy)_2(H_2O)]$	20.65	−13	[7]
$[Cu(NIT4Py)_2(DTB)_2(H_2O)_2]$	12.5	−8.89	this work

[a] δ is defined by the pyridine ring and ONCNO plane.

The $\chi_M T$ value at room temperature is 2.65 cm^3 mol^{-1} K for complex **2**, which is close to the spin-only expected value for two $S = 1/2$ and one $S = 3/2$ uncoupled spin systems (2.63 cm^3 mol^{-1} K). The $\chi_M T$ value at room temperature is 2.83 cm^3 mol^{-1} K for complex **4**, which is higher than the spin-only expected value for two $S = 1/2$ and one $S = 3/2$ uncoupled spin systems (2.63 cm^3 mol^{-1} K). When the systems are cooled down, the $\chi_M T$ value decreases. This implies the existence of weak antiferromagnetic spin exchange interactions both in complexes **2** and **4**.

The magnetic data were fitted into the isotropic model $\hat{H} = -2J(\hat{S}_{Co}\hat{S}_R + \hat{S}_{Co}\hat{S}_R)$, where J is the interaction parameter between two paramagnetic centers. For radical–Co(II)–radical complexes, the theoretical expression of the magnetic susceptibility is

$$\chi_M = \frac{N\beta^2 g^2}{4kT}\left[\frac{10 + \exp(-5J/kT) + 10\exp(-2J/kT) + 35\exp(3J/kT)}{2 + \exp(-5J/kT) + 2exp(-2J/kT) + 3\exp(3J/kT)}\right]$$

The best-fitted parameters were $J = -1.57$ cm^{-1}, $g = 2.01$, $R = 2 \times 10^{-5}$ for **2** and $J = -2.62$ cm^{-1}, $g = 2.02$, $R = 8.58 \times 10^{-5}$ for **4**, where R is defined as $R = \Sigma[(\chi_M)_{obs} - (\chi_M)_{calc}]^2/\Sigma(\chi_M)^2_{obs}$.

Those above results indicate that an antiferromagnetic exchange exists between the radical and metal ion.

For both complexes **2** and **4**, the magnetic exchange interactions between the Co(II) ion and the radicals are weak, which indicates the pyridine ring is not a suitable linker to transmit the magnetic interaction. Based on the orbital symmetry of the Co (II) ion of **2** and **4**, its two magnetic orbitals with σ symmetry ($d_{x^2-y^2}$, d_{z^2}) are orthogonal to the magnetic orbital (π^*) of the radical and would induce a ferromagnetic interaction, while its one magnetic orbital with π symmetry (either of d_{xy}, d_{xz}, d_{yz}) is able to overlap with the magnetic orbital of the radical to cause antiferromagnetic coupling. Meantime, due to the conjugation between the pyridine ring and the plane defined by five-atom fragment ONCNO, the unpaired electrons of the nitroxide radicals can delocalize onto the pyridine ring. The observed antiferromagnetic coupling in **2** and **4** can be attributed to the good overlap of the π^* magnetic orbital of the radical with the magnetic orbital with π symmetry of the Co (II) ion. Therefore, spin both on the Co (II) ion and the radical is expected to interact magnetically through the π-conjugated system, which leads to an antiferromagnetic interaction.

4. Conclusion

We have successfully obtained four new metal-radical complexes of the formula $[Cu(NIT3Py)_2(DTB)_2]$ **1**, $[Co(NIT3Py)_2(DTB)_2(CH_3OH)_2]$ **2**, $[Cu(NIT4Py)_2(DTB)_2(H_2O)_2]$ **3** and $[Co(NIT4Py)_2(DTB)_2(H_2O)_2]$ **4**. For the four complexes, the crystal structural analyses indicate that the two radical ligands are coordinated to the metal ions *via* the nitrogen atoms of the pyridine rings to form three spin complexes. All the complexes show weak antiferromagnetic interactions. A spin polarization mechanism and orbital symmetry are used to explain the magnetic properties of the four complexes. The values of the dihedral angles between the pyridyl ring and the nitroxide group of the radical would affect the magnetic properties in the four complexes. Although only weak antiferromagnetic interactions were observed in these compounds, our effort is to obtain single molecule magnets or single chain magnets with nitronyl nitroxide radicals. It is known that small changes in the coordination of the nitronyl nitroxide radicals and metal ions have a large influence on the magnetic properties of complexes. To realize our purpose, we are working on the synthesis of complexes with different metal ions and nitronyl nitroxide radical ligands.

Acknowledgements

This work was supported by the National Natural Science Foundation of China (No. 20771081 and No. 20771083)

Appendix A. Supplementary data

CCDC 629452, 629664, 746732 and 746733 contain the supplementary crystallographic data for this paper. These data can be obtained free of charge via www.ccdc.cam.ac.uk/conts/retrieving.html. Supplementary data associated with this article can be found, in the online version, at doi:10.1016/j.poly.2009.12.039.

References

[1] A. Caneschi, D. Gatteschi, A. Grand, J. Laugier, L. Pardi, P. Rey, Inorg. Chem. 27 (1988) 1031.
[2] H. Oshio, T. Watanabe, A. Ohto, T. Ito, H. Masuda, Inorg. Chem. 35 (1996) 472.
[3] J.-X. Xu, Y. Ma, D.-Z. Liao, G.-F. Xu, J. Tang, C. Wang, N. Zhou, S.-P. Yan, P. Cheng, L.-C. Li, Inorg. Chem. 48 (2009) 8890.
[4] N. Ishil, Y. Okamura, S. Chiba, T. Nogami, T. Ishida, J. Am. Chem. Soc. 130 (2008) 24.
[5] L.-C. Li, D.-Z. Liao, Z.-H. Jiang, S.-P. Yan, J. Chem. Soc., Dalton Trans. 1 (2002) 1.
[6] A. Cogne, J. Laugier, D. Luneau, P. Rey, Inorg. Chem. 39 (2000) 5510.
[7] H.-H. Lin, H.-H. Wei, G.-H. Lee, Y. Wang, Polyhedron 20 (2001) 3057.
[8] H. Oshio, T. Watanabe, A. Ohto, T. Ito, T. Ikoma, S.Tero-Kubota, Inorg. Chem. 36 (1997) 3014.
[9] Y. Ma, D.-Z. Gao, W. Zhang, K. Yoshimura, D.-Z. Liao, Z.-H. Jiang, S.-P. Yang, Inorg. Chim. Acta 14 (2006) 359.
[10] K. Hayakawa, D. Shiomi, T. Ise, K. Sato, T. Takui, J. Mater. Chem. 16 (2006) 4146.
[11] J.Tao, Y.-Z. Zhang, Y.-L. Bai, O. Sato, Inorg. Chem. 45 (2006) 4877.
[12] L.-Y. Wang, B. Zhao, C.-X. Zhang, Z.-H. Jiang, D.-Z. Liao, S.-P. Yan, Inorg. Chem. 42 (2003) 5804.
[13] R.-N. Liu, L.-C. Li, X.-Y. Xing, D.-Z. Liao, Inorg. Chim. Acta 362 (2009) 2253.
[14] J.-Y. Zhang, C.-M. Liu, D.-Q. Zhang, S. Gao, D.-B. Zhu, Inorg. Chim. Acta 360 (2007) 3553.
[15] R.P. Sharma, A. Singh, P. Branado, V. Felix, P. Venugopalan, J. Mol. Struc. 921 (2009) 227.
[16] D.-X. Hu, P.-K. Chen, F. Luo, L. Xue, Y. Che, L.-M. Zheng, Inorg. Chim. Acta 360 (2007) 4077.
[17] X. Wang, Y. Guo, E. Wang, L. Duan, X. Xu, C. Hu, J. Mol. Struc. 691 (2004) 171.
[18] Z.-L. Wang, L.-H. Wei, M.-X. Li, J.-P. Wang, J. Mol. Struc. 879 (2008) 150.
[19] E.F. Ullman, J.H. Osiecki, D.G.B. Boocock, R. Darcy, J. Am. Chem. Soc. 94 (1974) 7049.
[20] E.F. Ullman, L. Call, J.H. Osiecki, J. Org. Chem. 35 (1970) 3623.
[21] Siemens, SMART and SAINT, Area Detector Control and Integration Software, Siemens Analytical X-ray System, Inc, Madison, WI, 1996.
[22] G.M Sheldrick, SADABS Program for Empirical Absorption Correction of Area Dectector Data, University of Göttingen, Germany, 1996.
[23] G.M Sheldrick, SHELXS 97 Program for the Solution of Crystal Structure, University of Göttingen, Germany, 1997.
[24] G.M Sheldrick, SHELXL 97 Program for the Crystal Structure Refinement, University of Göttingen, Germany, 1997.
[25] H.M. McConnell, J. Chem. Phys. 39 (1963) 1910.
[26] T. Shimada, T. Ishida, T. Nogami, Polyhedron 24 (2005) 2593.
[27] H. Kumada, A. Sakane, N. Koga, H. Iwamura, J. Chem. Soc., Dalton Trans. (2000) 911.
[28] Y.-H. Xu, X.-N. Qu, H.-B. Song, L.-C. Li, Z.-H. Jiang, D.-Z. Liao, Polyhedron 26 (2007) 741.
[29] I. Dasna, S. Golhen, L. Ouahab, M. Fettouhi, O. Pena, N. Daro, J.-P. Sutter, Inorg. Chim. Acta 326 (2006) 37.
[30] S.-P. Wang, D.-Z. Gao, Y. Song, Z.-Q. Liu, D.-Z. Liao, Z.-H. Jiang, S.-P. Yan, Inorg. Chim. Acta 359 (2006) 505.
[31] L. Zhang, L.-C. Li, D.-Z. Liao, Z.-H. Jiang, S.-P. Yan, P.-W. Shen, Inorg. Chim. Acta 320 (2001) 41.
[32] L.-C. Li, D.-Z. Liao, Z.-H. Jiang, S.-P. Yan, Inorg. Chim. Acta 357 (2004) 405.